

HIRDLS

TC-RAL-047A

High Resolution Dynamics Limb Sounder

Originator: Martin Caldwell

Date: 5th Sep 94

Subject/Title: Ghost analysis results

Summary:

This note gives the results of the ghost analysis which was set out in TC-RAL-47, and it applies to baseline TC-RAL-33C .

The conclusion is that in this baseline ghost cross-talk levels are within the ITS out-of-field (OOF) specification, in all channels, at their respective 'cross-over' altitudes (that where the signal radiance drops to the 1/4 NEN level). These altitudes represent the 'most stringent case' conditions for vulnerability to ghost cross-talk.

In terms of contingency margin, the largest OOF ghost level is  $2.10^{-4}$ , about 20 times less than the OOF specification of 0.4%.

The results are based on an assumed anti-reflection coating reflectivity of 3% at all wavelengths.

Keywords: Ghost, results, cross-talk, filter spectral response, channel layout.

Purpose of this Document: Ghost results

(20 Characters Maximum)

Reviewed/approved by:			
Date:(day-mon-yr):			

Daresbury & Rutherford-Appleton Laboratory  
Chilton, DIDCOT, OX11 0QX  
United Kingdom

EOS

## Ghost analysis results.

### CONTENTS.

1. Results.
2. Notes on cross-talk calculations, (supplementary to TC-RAL-47).
  - 2.1 Spectral filter responses for  $S^{ji}$ .
  - 2.2 Optical path analysis for  $O^{ji}$ .
  - 2.3 Atmosphere matrix  $A^{ji}$ .
3. Conclusion
4. Future analyses.
  - 4.1 Data improvements.
  - 4.2 Design changes.
  - 4.3 Extending the analysis.
5. References.
6. Note on appendix format.
  - Appendix I Spectral matrix  $S^{ji}$ .
  - Appendix II Optical path matrix  $O^{ji}$ .
  - Appendix III Atmosphere matrix  $A^{ji}$ .
  - Appendix IV Ghost matrix  $g^{ji}$ .

### 1. Results.

This note presents the results of the ghost analysis which was set out in TC-RAL-47, and it applies to baseline TC-RAL-33C .

As previously explained, matrix formalism is used in the analysis, which is split into 3 main parts. These give three separate ‘cross-talk’ matrices, which describe

1. Spectral cross-talk (  $S^{ji}$  )
2. Optical path cross-talk (  $O^{ji}$  )
3. Atmosphere cross-talk (  $A^{ji}$  )

As the cross-talk is between 21 channels, the matrices are 21x21, and are given in appendices I, II, and III respectively. The net ghost matrix  $g^{ji}$  is an element-by-element multiplication of the three matrices, and this is given in appendix IV. The total ghost factor  $G^j$  in each signal channel  $j$  is the sum along the  $j$ 'th row of the matrix, i.e. the sum over all possible ghosting channels  $i$ . This parameter is compared directly with the OOF specification factor  $F=0.4\%$ , to ascertain compliance.

The results are given in table 1, where the compliance condition is that the values in the second column are less than one. Ghosting does not violate the specification in any channel. The largest ghost level is channel  $j=7$ , and this has a contingency margin equivalent to a factor of approximately 20.

Although only a minority of the 21x21 ghost cross-talk terms are found to be significant, the full matrices should be a useful reference for tracking or contemplating changes in design data, for example in the filter designs.

Signal channel $j$	ghost margin $G_j/F$ ( $F=0.4\%$ )
1	2.840E-5
2	8.978E-3
3	1.786E-2
4	8.605E-3
5	1.203E-2
6	2.090E-2
7	5.017E-2
8	5.169E-4
9	2.093E-3
10	3.3939E-6
11	1.5800E-3
12	2.9833E-4
13	1.8281E-4
14	1.3835E-3
15	9.0543E-3
16	1.6767E-2
17	6.7116E-3
18	5.2145E-3
19	4.1384E-4
20	4.1470E-4
21	1.3192E-5

Table 1. Ghost analysis results for all channels, in terms of the factor  $G^j/F$ , defined in TC- RAL-47, equation 12. **Compliance with specification is indicated by  $G^j/F < 1$ .**  
2. Notes on cross-talk calculations, (supplementary to TC-RAL-47).

### 2.1 Spectral filter responses for $S^{ji}$ .

The data on the cold (or focal plane) and warm (or secondary) filters (ref.1) was used as follows. The in-band filter response, i.e. the band-defining peak in transmission  $T$ , was extracted, out to the bandwidth where  $T$  drops to the background level. This level is determined by the blocking measurement confidence limit. For all other (out-of-band) wavelengths  $T$  is set equal to the background level. In these calculations the level was set at  $T=10^{-4}$ . This is thought to be a conservative figure for blocking, and it may later be revised downwards (ref.1).

In the spectral cross-talk matrix (appendix I) there is a large variation in element size, and the data is given in log form. The largest terms are those close to the main diagonal, representing the spectrally adjacent channels having significant overlap (channels are numbered in wavelength order). Away from the main diagonal the  $S^{ji}$  are small, at a background level determined mainly by the assumed blocking level given above.

### 2.2 Optical path analysis for $O^{ji}$ .

This part of the analysis is done using a ray-trace in the ASAP program, relying on ray flux monitoring, and ray-splitting at interfaces according to coating properties (mainly the anti-reflection AR coatings).

As previously explained, the main analysis is for first-order ghosts involving only one AR coating reflection at one of six possible surfaces. The analysis is begun using 50,000 signal rays, generating an additional 300,000 ghost rays in the trace. A longer run using 150,000 signal rays was also done, for one channel only, as a check on the ray sampling accuracy.

An example ghost trace spot diagram is shown figure 1. For ray-sampling reasons, the ghost ray fluxes are summed over an area equivalent to the cold filter apertures (shown in the diagram), although this is about 3 times larger than the intended warm filter area. Since the ghost rays are spread reasonably uniformly, a simple area correction can be applied for the actual intended warm filter aperture. The warm filter oversize assumed is, with respect to the detector image size, 20% in radius in the vertical direction (TC-RAL-47). Horizontally the radius oversize is the same in absolute terms as the value derived for the vertical.

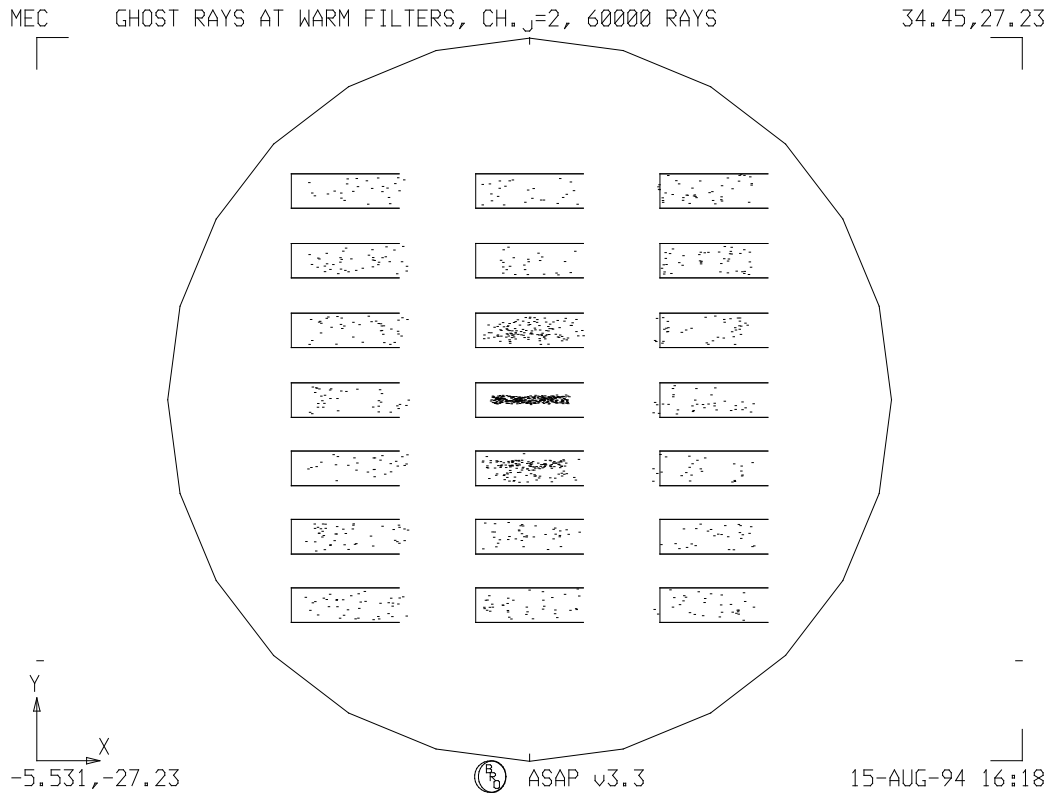
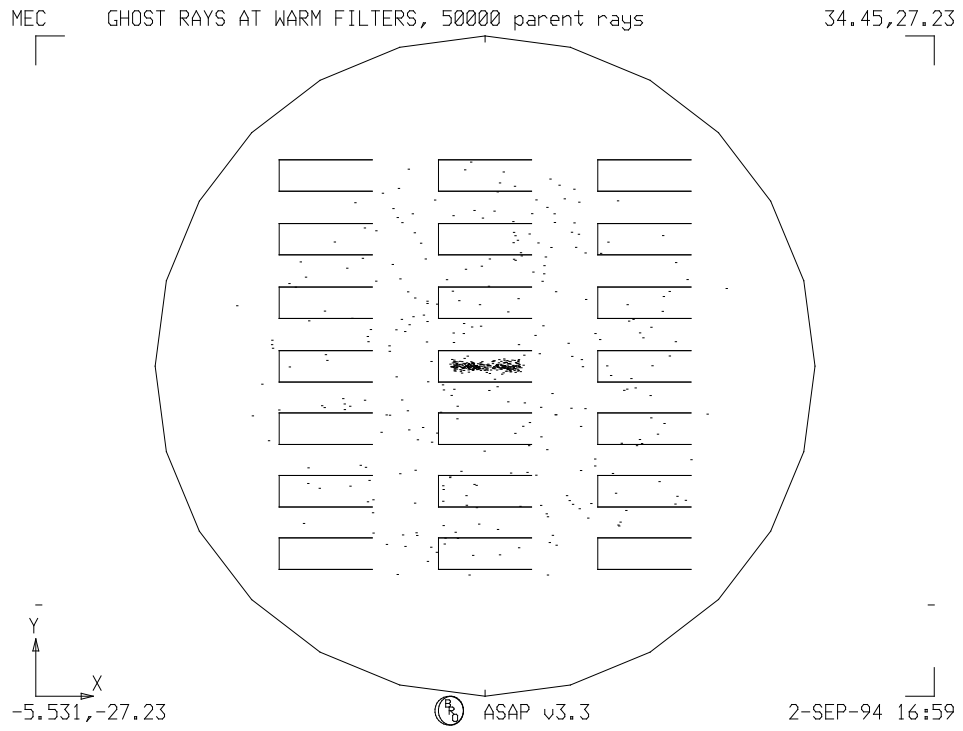


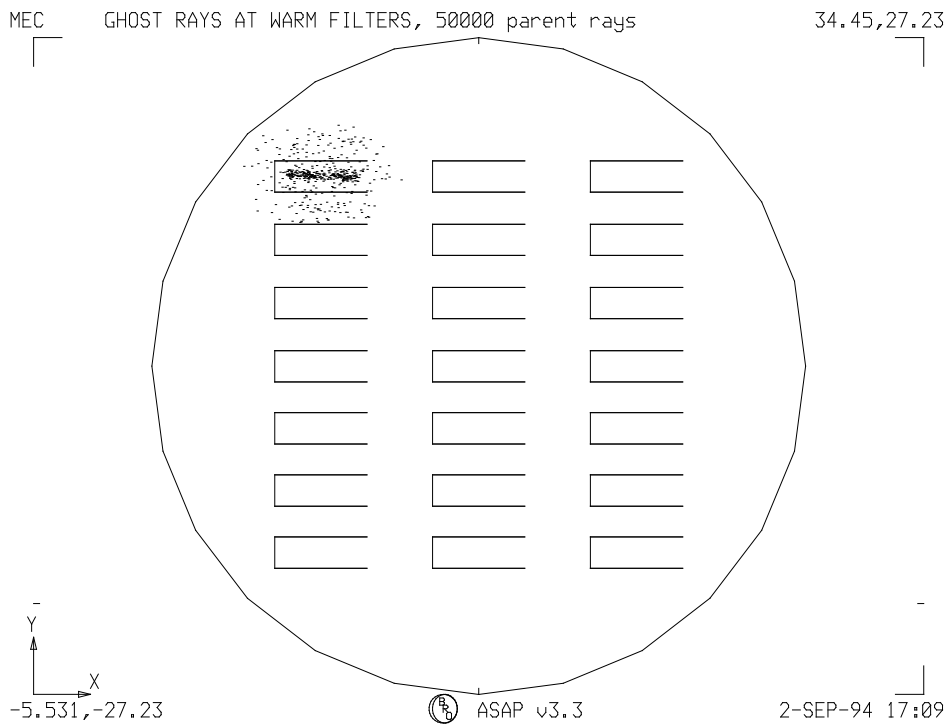
Figure 1. Example spot diagram for first-order ghost rays.

The statement in TC-RAL-47 on second order ghost paths, i.e. those involving two AR coating reflections, was that because these contain rays with lower flux, they would only be significant where they are strongly focused. Such second-order paths cannot be included with the main first-order ray-trace (figure 1), because they require two ‘generations’ of ghost rays, leading to an explosion in the ray population beyond the practical limit. This problem is overcome by describing the second order ghosts individually them separate traces.

The focusing of these potential ‘double-bounce’ ghosts was checked by Ian Tosh using the CODEV program. Two cases showed sufficient focusing to warrant the full analysis with ASAP. These were the double reflection within the first lens, and that within the dewar window. The spot diagrams for these are shown in figure 2.



(a)



(b)

Figure 2 Spot diagrams for second-order ghost paths

- (a) Double reflection in first lens
- (b) Double reflection in dewar window.

The lens ghost is de-focused to a beam with a diameter similar to that of the array. The ghost level which this produces is similar in all channels, and is about ten times smaller than the typical level from the first order paths (figure 1).

The dewar window ghost is more tightly focussed, but to such an extent that it doesn't spill into neighbouring channels. Consequently the contribution to ghost cross-talk is negligible. However, this ghost could have a significant effect on vertical response profile, and it will also be analysed in that context.

The present ghost analysis does not include the optical throughput factors for each channel. (These were calculated for example in TC-RAL-037 and 039, for previous baselines.). The main effect involved is that of optical absorption in the lens and window materials, and this could be incorporated into the ASAP description for any later analysis. The effect of absorption is to reduce the relative ghost level rather than increase it. This is because most ghost optical paths involve multiple passes through the absorptive elements, as opposed to single passes for the signal paths, and so they will experience greater absorption. Hence with absorption included, the ghost levels of table 1 would be improved somewhat.

### 2.3 Atmosphere matrix $A^{ji}$ .

The atmosphere cross-talk matrix is listed in appendix III. As detailed in TC-RAL-47, the elements  $A^{ji}$  are radiance ratios. Element (j,i) is the signal channel radiance  $B^j$  at the signal altitude  $h^j$ , divided into the value of  $B^j$  at the altitude  $h^i$  of the i'th ghosting channel, i.e.

$$A^{ji}(h^j) = \frac{B^j(h^i)}{B^j(h^j)}$$

(TC-RAL-47, equation (14) ).

$A^{ji}$  is evaluated at a different height for each signal channel j. The height chosen is the most stringent case, that of the cross-over altitude ( $h_{lim}^j$  in TC-RAL-47) where the signal has decreased to the 1/4.NEN value. The  $A^{ji}$  matrix has been calculated from the atmosphere data of TC-HIR-90 review A , in combination with the baseline detector layout.

There are several points to note about the values of  $A^{ji}$  in appendix III.

1. Where  $A^{ji} = 1$ , this occurs because the channels share the same altitude position in the array.
2. The ghost problem arises from channels i which are at lower altitudes than the signal channel j, and so may be much brighter ( $A^{ji} \gg 1$ ). The contribution from channels i at altitudes higher than channel j is negligible and has not been computed, leading to

zeros in the matrix. Thus where  $A^{ji} = 0$ , the implication is that channel  $i$  is above channel  $j$  in the array. In reality this gives  $A^{ji} < 1$ , and the assumption is that the contribution to ghosting is then negligible.

3. For a signal channel  $j$  with a cross-over altitude  $< 55\text{km}$ , some of the ghosting channels  $i$  may have negative altitude, i.e. they lie on the earth disc. The radiance value then used in the calculation is the  $j$  atmosphere radiance at zero altitude. I.e. for decreasing altitude the scene radiance is assumed to be continuous at  $h^j = 0$ , and constant thereafter for  $h^j < 0$ .
4. In some discussions of ghosting, the relevant variation of atmosphere brightness with altitude has been taken to be about three orders of magnitude, a figure probably derived from inspection of the radiance data alone. The largest values of  $A^{ji}$  are actually much less than this (in fact  $A^{ji} < 10^2$ ), because of the limited vertical field, and the careful design of the new channel layout. The vertical full field dimension is limited to  $55\text{km}$ ; ghost sources beyond this field are not admitted by the warm filter mask.

### 3. Conclusion.

A full ghost analysis has been completed. This is ‘full’ in the sense that the three causes of the problem are all properly included. These are spectral overlap of channels, optical ghost paths, and scene (atmosphere) non-uniformity.

The matrix formalism for separating the analysis into these three parts was given in TC-RAL047, and additional assumptions used in the calculations were also given here. This separation of the analysis will minimise the extra work required for any further analyses or design changes.

All of the possible cross-talk terms have been computed (appendices I to IV), and these provide look-up tables for easy detection of the problem cases.

The final results (table 1) show compliance with the ITS requirement, with a provisionally acceptable margin ( a factor of 20).

### 4. Future analyses.

As the instrument design and the stray light budgets become established in more detail, re-runs of the ghost model may be required to check the various changes. These are likely to include the following.

#### 4.1 Data improvements.

These should include:

- Absorption (throughput) data for lens and window materials.
- Anti-reflection coating data across the full HIRDLs waveband.
- Better earth radiance estimates.

#### 4.2 Design changes.

Areas of change which affect ghosting include:

- Lens forms (choice of surface for aspheric), affecting  $O^{ji}$ .
- Filter design (warm filters), affecting  $S^{ji}$ .

#### 4.3 Extending the analysis.

The following analyses may eventually be required:

- Ghost level calculations over full altitude range (requiring re-runs of  $A^{ji}$  only), to demonstrate full compliance with the specification.
- Modelling of filters as two-surface components, possible if the filter data can be extended likewise.
- Consideration of ghost budget de-scoping to allow other stray light effects to have larger budget.

#### 5. References.

1. Infra-Red Multi-layer Lab, Dept. of Cybernetics, University of Reading.  
Filter data and blocking discussions with Roger Hunneman, data files provided by Gary Hawkins.

#### 6. Note on appendix format.

The following appendices list the 21x21 matrices for the ghost cross-talk terms. Due to page width and text format limitations in the ASAP program, the matrices have been printed in segments, each of size 7x7. The relevant (j,i) values are given in each table, but it is useful to also understand the ordering of the segments as printed here. The header of each table quotes a 'page (segment) number' and this relates to the 21x21 matrix with the format shown in figure 3.

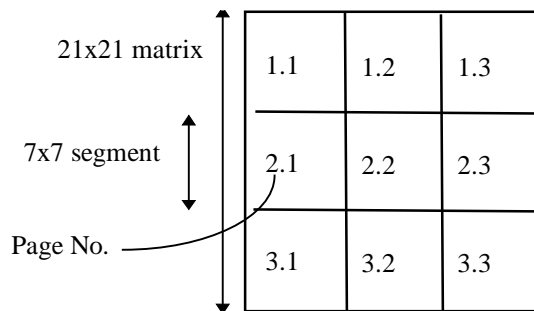


Figure 3 Page format for matrix listing in appendices.

The order in which the pages are listed is

- 1.1
- 1.2
- 1.3
- 2.1 ... etc.